

IL NUOVO CIMENTO 41 C (2018) 101

DOI 10.1393/ncc/i2018-18101-1

COMMUNICATIONS: SIF Congress 2017

Recent R&D to improve the time resolution and rate capability of the Multigap Resistive Plate Chamber

F. CARNESECCHI⁽¹⁾⁽²⁾⁽³⁾^(*)

⁽¹⁾ *Centro Fermi, Museo Storico della Fisica e Centro Studi e Ricerche “Enrico Fermi”
Rome, Italy*

⁽²⁾ *Dipartimento di Fisica e Astronomia, Università di Bologna - Bologna, Italy*

⁽³⁾ *INFN, Sezione di Bologna - Bologna, Italy*

received 24 January 2018

Summary. — In this study the results of tests performed at the T10 beam line at CERN on three novel MRPC detectors are reported. The tested detectors have different designs suited for different R&D goals: one detector has been built to improve the already excellent time resolution of the MRPC technology; the other two detectors have been designed and constructed to improve the MRPC rate capabilities. All the detectors are built maintaining the basic features of MRPCs: low price and ease of construction. The solutions adopted and described in this work for the time resolution improvement lead to a detection efficiency close to 100%, demonstrating the chamber functionality. To increase the MRPCs rate capabilities, a painted layer has been added to the surfaces of the MRPCs inner glass sheets. The measurements and tests performed showed that this solution can indeed increase the rate capability of the detector with respect to standard MRPC.

1. – Introduction

The Multigap Resistive Plate Chamber (MRPC) [1] is a gaseous detector with excellent efficiency ($> 95\%$) and time resolution (~ 50 ps). Thanks to these characteristics, these detectors are used in various experiments, such as: ALICE [2], EEE [3], FOPI [4], HADES [5], HARP [6] and STAR [7].

Even though the MRPC is a cutting-edge detector, *R&D* is still important and necessary in view of the next generation of colliders such as HL-LHC [8] and FCC [9]; in particular a detector with a time resolution of tens of picosecond and the capacity to withstand an high rate of particles can be a perfect candidate for such a hostile environment.

^(*) E-mail: francesca.carnesecchi@bo.infn.it

1.1. *R&D: improving time resolution.* – Nowadays the MRPC can achieve a time resolution of 40–50 ps, inclusive of the whole electronic chain. What is known is that an MRPC intrinsic time resolution better than 20 ps is possible [10]; nevertheless what is not trivial is trying to get the same performances keeping the low cost and ease of construction typical of the MRPC, while minimising the quantity of dense material⁽¹⁾. To test this possibility an MRPC has been designed and built to improve the time resolution. The chamber has been built with a great number of thin gas gaps using a simpler configuration than that described in [10].

1.2. *R&D: improving rate capability.* – The MRPC limited rate capability has also been investigated; indeed the MRPC, built with sheets of soda-lime glass ⁽²⁾, with a bulk resistivity $\rho = 5 \cdot 10^{12} \Omega \text{ cm}$, has a rate capability limited to about 1 kHz/cm². As explained in [11-13], the high resistivity of the glass plates is the main limiting factor for the rate capability; the voltage drop ΔV per unit area is given by the charge (Q) collected on the resistive plate of thickness (s), multiplied by the number of plates (n) and the flux of particles through the detector:

$$(1) \quad \Delta V = n s Q \rho \text{ Rate}$$

thus $\Delta V \propto \rho \cdot \text{Rate}$. The clear inference is that by reducing the resistivity the rate can be increased. There are indeed low-resistivity glass sheets and ceramics being studied as resistive plates for high rate applications [14]; nevertheless this kind of electrodes introduce some difficulties: they are not easily produced (not common) and, as a consequence, the price is high. In this work two chambers have been designed and built with an alternative approach: instead of replacing the electrode, the idea was to add a painted layer on the internal soda-lime glass sheets. For these internal resistive painted surfaces, the surface resistivity would be lower, the charge will evacuate faster resulting in an increase of the rate capability. A theoretical study has been made by Riegler [15].

2. – Construction

All the three chambers have been built using the same basic materials. They consist of stacks of glass sheets of 280 μm thickness and $5 \cdot 10^{12} \Omega \text{ cm}$ bulk resistivity. The glass sheets, of $20 \times 20 \text{ cm}^2$ active area, were cut from a glass sheet of $\sim 1 \text{ m}^2$. The outer surface of the external glass sheets has been coated with a resistive paint of $5 \text{ M}\Omega/\square$; they work as electrodes where the high voltage is applied.

The spacers between two glass sheets are mono-filament commercial fishing lines of different diameters (gas gap thickness) depending on the chamber; the fishing lines are stretched across the surface of the glass from one side to the other and around plastic screws fixed along both sides of the chamber. In fig. 1 (left) a picture of a chamber during the assembling is reported; the fishing lines stretched across the glass sheets are visible.

The Printed Circuit Boards (PCB) are 1.5 mm thick and insulate 24 readout strips from the anode and cathode electrodes; the strips are $(0.7 \times 20.5) \text{ cm}^2$, separated by

⁽¹⁾ This would be important in an experiment with a calorimeter downstream of the MRPC, so that through-going particles lose the smallest amount of energy.

⁽²⁾ AGC glass sheets.

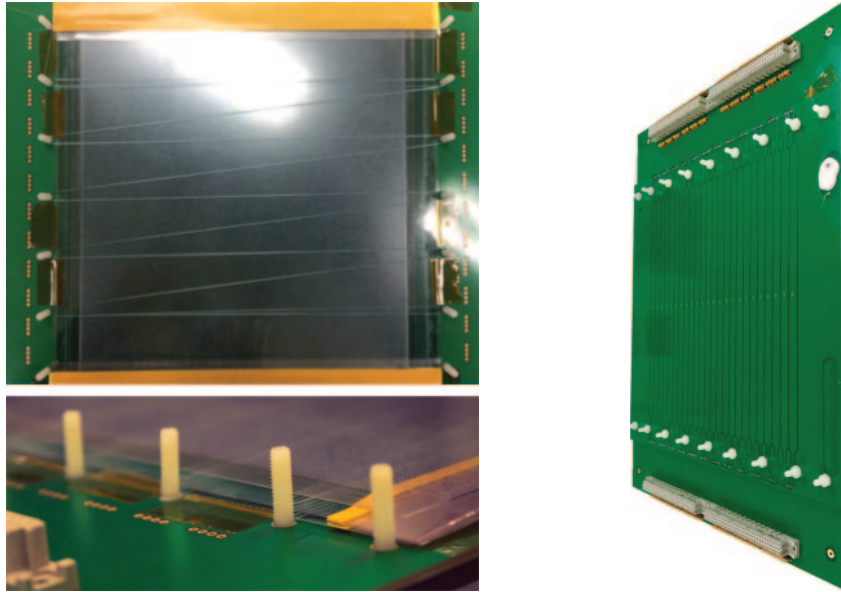


Fig. 1. – Two pictures of a chamber during the assembling of the chamber: a top and a lateral view (left). A picture of the PCB used during the assembling (right).

1 mm. In fig. 1 (right) a picture of the PCB is shown; the 24 readout strips and the connectors for the front-end electronics (in grey) are visible. Each strip is read out at both ends of the strip (to improve the time resolution, avoiding the broadening due to the hit position).

The anode and cathode boards are connected by pins that attach the PCBs together; thus a differential signal is sent to the front end. A honeycomb panel is attached to the PCBs with a double-sided adhesive tape, to ensure the rigidity of the structure. The chamber is finally enclosed in a gas-tight aluminium box and flushed with a gas mixture of $C_2H_2F_4$ and SF_6 .

Due to the different foreseen applications of the chambers the number of stacks, gas gaps and thickness are different.

2'1. *MRPC(20/180)*. – This chamber has been built for ultra-precise timing purposes with a total of 20 gas gaps of $180\ \mu m$ thickness; a double-stack configuration has been used, with 10 + 10 design, with a total of 3 PCBs. In fig. 2 (left) a schematic view of the chamber is shown.

2'2. *MRPC(4/300)* and *MRPC(5/250)*. – Two different chambers have been built for the rate capability study with two different design; both are single-stack configuration, each using a total of 2 PCBs. For the *MRPC(4/300)* an internal painted layer has been added on both surfaces of each glass sheet; for the *MRPC(5/250)* an internal painted layer has been added on the cathode side of each glass sheet. See fig. 2 (right) for a schematic view of the chamber. The internal painted layer has a resistivity of $100\ M\Omega/\square$.

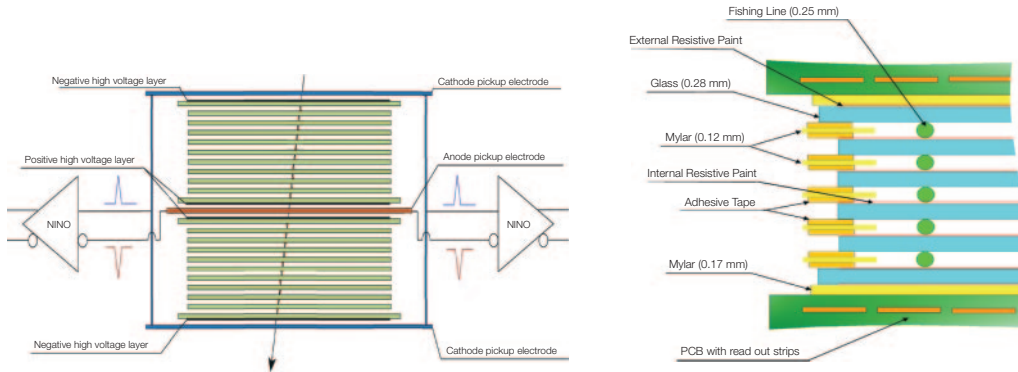


Fig. 2. – Schematic view of the design of the MRPC(20/180), the double-stack structure is shown together with an inner positive high-voltage layers, and two external negative high-voltage layers (left). Schematic view of MRPC(5/250) with construction details (right).

3. – Experimental setup

The MRPCs have been tested at the T10 test beam line at CERN. The beam was composed mainly of negative pions of $5 \text{ GeV}/c$ momentum. The gas mixture was $\text{C}_2\text{H}_2\text{F}_4$ (95%) and SF_6 (5%) with a continuous flow of 51/h. For the rate capability measurements, it is of particular importance to point out that a spot illumination in a pulsed beam was used: there were 2 spills (400 ms long) per PS supercycle that had a period of approximately 22 s; this situation is different from a flood illumination.

In fig. 3, a schematic view of the experimental setup is shown. Three sets of scintillators coupled to photomultipliers have been used for the trigger. In particular, starting from the beam entrance, the first set ($S1-S2$, $S3-S4$) consists of two orthogonal scintillator bars of $(2 \times 2 \times 10 \text{ cm}^3)$, read at each end by photomultipliers. The second set is made of a pair of crossed scintillators ($P1-P2$) with a crossed area of $1 \times 1 \text{ cm}^2$, read by photomultipliers. Next there is the MRPC under test and finally the last pair of crossed scintillators ($P3-P4$), with a crossed area of $2 \times 2 \text{ cm}^2$, read by photomultipliers.

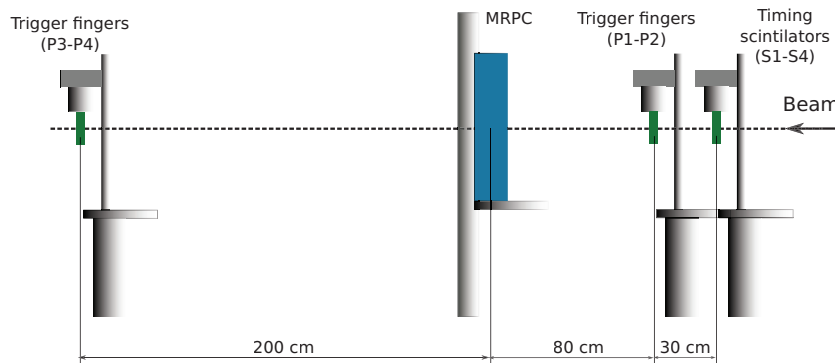


Fig. 3. – Schematic view of the experimental setup at CERN T10; the three sets of scintillators coupled to photomultipliers used for the trigger are visible.

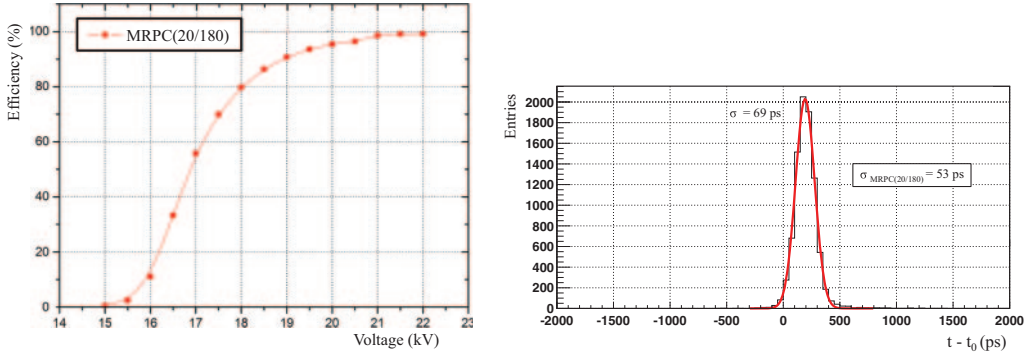


Fig. 4. – The efficiency as a function of the applied voltage (left) and the time resolution at 21 kV (right) for the MRPC(20/180). The errors bars are contained within the symbol size.

$S1$ - $S2$, $S3$ - $S4$ are also used as timing reference, t_0 , by means of the average between all the detectors $((S1+S2+S3+S4)/4)$. A t_0 time resolution of 40–50 ps has been estimated by inspection of the time difference between the two bars, *i.e.* $((S1+S2)/2 - (S3+S4)/2)$.

The strips were read out at both ends using 24 Channels NINO ASIC cards [16, 17]. The data were taken using two CAEN HPTDCs (V1290 A) with a bin size of 25 ps; the HPTDC time resolution is (20–30) ps.

4. – Results and discussion

4.1. *MRPC(20/180)*. – This chamber was built with the aim of improving the time resolution maintaining other MRPC characteristics. The efficiency as a function of the applied voltage has been measured. As shown in fig. 4 (left), an efficiency of almost 100% at a voltage of 21 kV has been reached. The dark current as a function of applied voltage has been also measured; as expected, it increases with voltage reaching 200 nA at 22 kV.

As second step, the time resolution of the detector was investigated. In fig. 4 (right) an histogram of the time difference measured between the MRPC(20/180) and the reference scintillators is shown. To get the final time resolution the jitter of the scintillators ($\sigma_{t_0} = 44$ ps) has been quadratically subtracted, resulting in a time resolution of (53 ± 1) ps.

From the results on efficiency and (dark) current, it can be concluded that the chamber is perfectly working, with a low current and a high efficiency; moreover, with our design, the difficulties on the construction (reduced number of stacks), the price (less material) and a lower material budget (a total of three PCBs have been used together with a smaller number of thinner glass sheets), compared to a previous work [10].

It should be pointed out that the reported time resolution includes the full chain of front end and readout electronics, whose contribution dominates the results.

The next step, after this first testing stage, would be to test the chamber with an appropriate readout electronics, with a much smaller time jitter, *e.g.* an oscilloscope (as in [10]), in order to measure the intrinsic time resolution of the MRPC(20/180).

4.2. *MRPC(4/300) and MRPC(5/250)*. – These chambers were built with different designs and with the aim of improving the MRPC rate capability; as mentioned, a spot illumination in a pulsed beam has been used (however the comparative rate reflects the intrinsic rate capability of the various MRPCs). With high rates a degradation of both

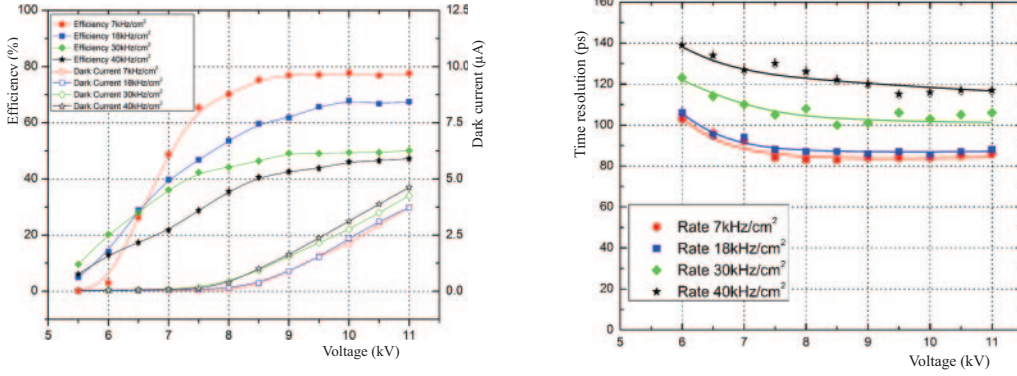


Fig. 5. – Efficiency, dark current (left) and time resolution (right) *vs.* the voltage as a function of the rate of particles for MRPC(4/300), the double side painted. The errors are contained within the symbol size.

the efficiency and time resolution is expected for standard MRPC. This can be observed in [18] where the results of a test on a standard MRPC (without any inner painted layer added), MRPC-1, are reported. The chamber was a six gas gaps of $220\ \mu\text{m}$ width. The results for MRPC-1 can be used as comparison for MRPC(4/300) and MRPC(5/250).

To test the chambers MRPC(4/300) and MRPC(5/250), the rate of particles provided by the T10 beam line has been increased; the aim was to measure the efficiency, the dark current and the time resolution as a function of the applied high voltage and for increasing values of rate. The T10 trigger (see previous section) has been used to monitor the rate; the beam intensity has been changed by modifying the collimator aperture. Four different rates have been tested, from $7\ \text{kHz}/\text{cm}^2$ to $40\ \text{kHz}/\text{cm}^2$.

In fig. 5 the results for the MRPC(4/300), the double-side painted, are reported; in particular the efficiency, current and time resolution *vs.* the voltage, for the various rates, are shown. In fig. 6, the same kind of plots for MRPC(5/250), the single-side painted, are shown.

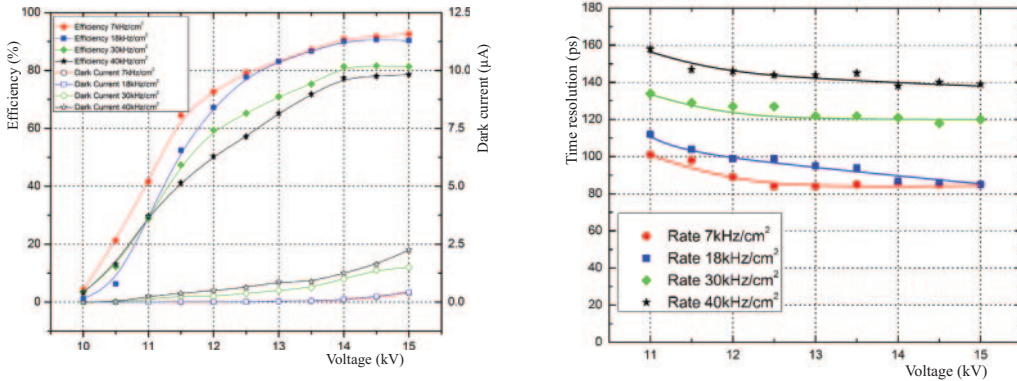


Fig. 6. – Efficiency, dark current (left) and time resolution (right) *vs.* the voltage as a function of the rate of particles for MRPC(5/250), the one side painted. The errors are contained within the symbol size.

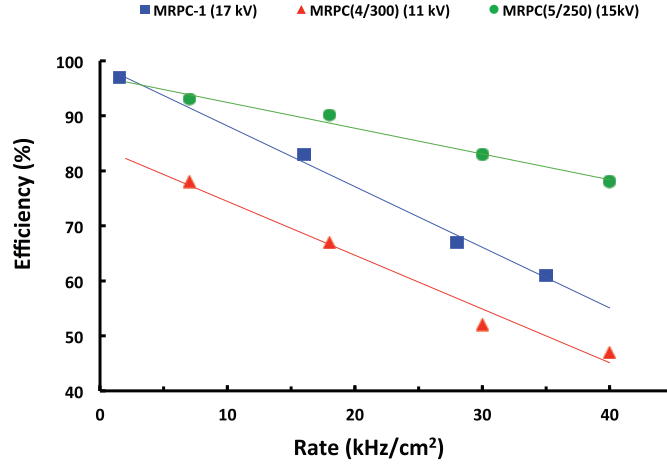


Fig. 7. – The efficiency *vs.* the rate at a plateau voltage for a standard chamber MRPC-1 (with 6 gas gap of $220\ \mu\text{m}$) and the two chambers tested, MRPC(4/300) (double-side painted) and MRPC(5/250) (one-side painted). The errors are contained within the symbol size.

At the rate of $7\ \text{kHz}/\text{cm}^2$, the MRPC(4/300) reaches the plateau at $\sim 9\ \text{kV}$ with an efficiency of $\sim 78\%$; the MRPC(5/250) reaches the plateau at $\sim 14\ \text{kV}$ with an efficiency of $\sim 93\%$. These differences plateau voltages are just due to the different thickness and number of gaps.

Moreover, the plots show the clear dependence of the efficiency and time resolution with the rate for both detectors. It is interesting to compare the present results with those of a standard MRPC [18]. In the standard chamber, starting from a rate of $1.5\ \text{kHz}/\text{cm}^2$ to $35\ \text{kHz}/\text{cm}^2$, at $16.5\ \text{kV}$, there is a degradation of $\sim 38\%$ in efficiency and $\sim 44\%$ in time resolution.

In MRPC(4/300) the degradation at $11\ \text{kV}$ are of $\sim 40\%$ and $\sim 30\%$ for efficiency and time resolution, respectively; while in MRPC(5/250), at $15\ \text{kV}$, a degradation of $\sim 15\%$ for efficiency and of $\sim 39\%$ for time resolution, is observed.

The results have been obtained keeping the low-cost requirement and ease of construction of the MRPCs. Concerning the time resolutions, the same behaviour of the standard MRPC have been observed.

It can be noticed that the expected better results for the double-sided painted MRPC (4/300) compared to the MRPC(5/250), have not been observed. A possible explanation is that the *hand* painting of the inner glass sheets can lead to some non uniformity on the thickness of the painted layer; this can affect the results. Anyway, to fully compare them, two identical chambers, except for the different way of painting, should be built.

The results here presented, that are a first stage of this *R&D* in rate capabilities improvements for MRPC, demonstrate that the principle is working; indeed in MRPC(5/250) a lower degradation of efficiency with increasing rate has been observed compared to standard MRPCs. In fig. 7 the final results on efficiency are highlighted. The final step will be then to have a *factory-painted* glass sheets and repeat the tests.

* * *

This work was supported by the ALICE-TOF R&D, under the guidance of Dr. M. C. Williams.

REFERENCES

- [1] CERRON ZEBALLOS E. *et al.*, *Nucl. Instrum. Methods A*, **374** (1996) 132.
- [2] DELLACASA G. *et al.*, *ALICE technical design report of the time-of-flight system (TOF)*, CERN-LHCC-2000-012 (2000).
- [3] ABBRESCIA M. *et al.*, *Eur. Phys. J. Plus*, **128** (2013) 62.
- [4] SCHÜTTAUF A. *et al.*, *Nucl. Instrum. Methods A*, **602** (2009) 679.
- [5] BELVER D. *et al.*, *Nucl. Instrum. Methods A*, **602** (2009) 687.
- [6] AMMOSEV V. *et al.*, *Nucl. Instrum. Methods A*, **602** (2009) 639.
- [7] BONNER B. *et al.*, *Nucl. Instrum. Methods A*, **478** (2002) 176.
- [8] APOLLINARI G. *et al.*, *High-Luminosity Large Hadron Collider (HL-LHC)*, Preliminary Design Report, CERN Yellow Reports, Monographs (2015) <http://cds.cern.ch/record/2116337>.
- [9] BENEDIKT M. and ZIMMERMANN F., *Future Circular Colliders*, in *Proceedings of the International School of Physics "Enrico Fermi"*, Vol. **194** (IOS Press; SIF) 2016, pp. 73–80.
- [10] AN S. *et al.*, *Nucl. Instrum. Methods A*, **594** (2008) 39.
- [11] LIPPMANN C. *et al.*, *Nucl. Phys. B, Proc. Suppl.*, **158** (2006) 127.
- [12] ABBRESCIA M., *Nucl. Instrum. Methods A*, **533** (2004) 7.
- [13] GONZALEZ-DIAZ D. *et al.*, *Nucl. Phys. B, Proc. Suppl.*, **158** (2006) 111.
- [14] DEPPNER I. *et al.*, *Nucl. Instrum. Methods A*, **661** (2012) 121.
- [15] RIEGLER W., *JINST*, **11** (2016) P11002.
- [16] ANGHINOLFI F. *et al.*, *Nucl. Instrum. Methods A*, **533** (2004) 183.
- [17] ANGHINOLFI F. *et al.*, *IEEE Trans. Nucl. Sci. Proc.*, **51** (2004) 1974.
- [18] FORSTER R. *et al.*, *Nucl. Instrum. Methods A*, **830** (2016) 182.